RSC Advances

PAPER

View Article Online
View Journal | View Issue

Cite this: *RSC Adv.*, 2022, **12**, 23566

Fabrication of hydrolase responsive diglycerol based Gemini amphiphiles for dermal drug delivery applications†

Ayushi Mittal,[a] Krishna,[a] Fatemeh Zabihi,[bc] Fiorenza Rancan,[b] Katharina Achazi,[c] Chuanxiong Nie,[c] Annika Vogt,[b] Rainer Haag[c] and Sunil K. Sharma *[a]

Since biocatalysts manoeuvre most of the physiological activities in living organisms and exhibit extreme selectivity and specificity, their use to trigger physicochemical change in polymeric architectures has been successfully used for targeted drug delivery. Our major interest is to develop lipase responsive nanoscale delivery systems from bio-compatible and biodegradable building blocks. Herein, we report the synthesis of four novel non-ionic Gemini amphiphiles using a chemo-enzymatic approach. A symmetrical diglycerol has been used as a core that is functionalised with alkyl chains for the creation of a hydrophobic cavity, and for aqueous solubility (polyethylene glycol) monomethyl ether (mPEG) is incorporated. Such systems can exhibit a varied self-assembly behaviour leading to the observance of different morphological structures. The aggregation behaviour of the synthesised nanocarrier was studied by dynamic light scattering (DLS) and critical aggregation concentration (CAC) measurements. The nanotransport potential of amphiphiles was investigated for hydrophobic guest molecules, *i.e.* Nile red, nimodipine and curcumin. Cytotoxicity of the amphiphiles was studied using HeLa and MCF7 cell lines at different concentrations, *i.e.* 0.05, 0.1, and 0.5 mg mL^{-1}. All nanocarriers were found to be non-cytotoxic up to a concentration of 0.1 mg mL^{-1}. Confocal laser scanning microscopy (cLSM) study suggested the uptake of encapsulated dye in the cytosol of the cancer cells within 4 h, thus implying that amphiphilic systems can efficiently transport hydrophobic drug molecules into cells. The biomedical application of the synthesised Gemini amphiphiles was also investigated for dermal drug delivery. In addition, the enzyme-mediated release study was performed that demonstrated 90% of the dye is released within three days. All these results supported the capability of nanocarriers in drug delivery systems.

Received 16th May 2022
Accepted 5th August 2022

DOI: 10.1039/d2ra03090j

rsc.li/rsc-advances

1. Introduction

Stimuli responsive polymers which are sometimes classified as "smart" or "intelligent" materials have become increasingly popular over the last three decades as they are known to exhibit dramatic behaviour. They may be associated physically or chemically with a variety of bio-active molecules to control the expression of characteristic behaviour of these molecules.[1,2]

The hydrolase responsive polymeric systems in this endeavour hold promise as mild exposure with the biocatalyst may be instrumental for physicochemical changes in the polymeric architecture.[3] As a part of our ongoing research to evolve various value added products from glycerol, a by-product of oleochemical and biodiesel industry,[4] herein, we have used a linear dimer of glycerol (diglycerol) to develop an amphiphilic system for dermal delivery applications.

Dermal drug delivery is an upcoming area and being used as an effective alternative to the oral drug delivery and hypodermic injections. It offers the release of the drug into systemic circulation through the skin in a controlled manner which can avoid the first pass metabolism, reduce the invasion of external molecules, avoid gastrointestinal absorption and reduce side effects. For the dermal drug delivery, skin is considered to be a relevant target because it is the main barrier against external circumstances and also prevents the penetration of chemical and biological agents. Skin is the vastest and complex organ of the human body and occupies a surface area of about 1.5–2.0 m^2. It serves as a protecting barrier against external circumstances along with the prevention of the penetration of chemical and biological agents. Its outermost layer, *i.e.* stratum corneum is composed of corneocytes only and permeable to small sized (~500 Da) neutral molecules having a low melting point. Previous studies have established that only small

[a]*Department of Chemistry, University of Delhi, Delhi 110 007, India. E-mail: sk.sharma90@gmail.com; Tel: +91-11-27666646*
[b]*Clinical Research Center for Hair and Skin Science, Department of Dermatology and Allergy, Charité – Universitätsmedizin Berlin, Charitéplatz 1, 10117 Berlin, Germany*
[c]*Institut für Chemie und Biochemie, Freie Universität Berlin, Takustraße 3, 14195 Berlin, Germany*

† Electronic supplementary information (ESI) available. See https://doi.org/10.1039/d2ra03090j

hydrophobic molecules can pass across the extracellular lipid membrane of the skin.[5–8] Hence, a wide variety of nanoscale carriers have been developed to facilitate the efficient delivery of various therapeutics across the barriers in which amphiphilic nanocarriers are of great interest. Also, the amphiphilic nanocarriers are known for their enhanced permeability and retention (EPR) effect which also enhances the cargos stability, bioavailability, blood circulation time and their tumour targeting ability.[9–11]

Self-assembly of amphiphiles is a spontaneous organization of disordered building blocks, which is governed by specific mutual interactions and it produces a variety of assemblies, which depend upon the molecular structure of the amphiphiles.[12–15] Singh *et al.* reported the aggregation behaviour of twinned amphiphiles synthesised using A_2B_2 spacer and demonstrated various self-assemblies such as globular, thread-like micelles, ribbon like, rod like and planar double layer assemblies by varying the length of hydrophilic PEG and hydrophobic alkyl chains.[16] In 2015 Zheng *et al.* reported Gemini supra-amphiphiles which self-assemble into vesicles, nanotubes and planar bilayers by varying the length of the spacer.[1] Among the broad classification of amphiphiles, the well known Gemini amphiphiles have attracted considerable attention due to their self-assembly behaviour. Gemini amphiphiles consists of two polar (hydrophilic) head groups and two non-polar (hydrophobic) tail groups which are covalently attached *via* the spacer.[17] The presence of two hydrophobic tails allows Gemini amphiphiles to have lower CAC, surface tension, minimal inhibitory concentration (MIC), and Krafft temperature values than the conventional monomeric surfactants.[18,19] Moreover, the balance between lipophilic and hydrophilic units and the position of spacer between them controls the pre-organization of molecules in water, resulting in various morphological structures like spherical, ellipsoidal, rod shape, ribbons, micellar threads, globular micelles, *etc.*[16]

Herein, we synthesised Gemini amphiphiles, where a symmetrical diglycerol was used as a core and it also acts as a spacer between the hydrophobic alkyl chains. The self-assembly behaviour of these amphiphiles in aqueous medium and their drug delivery potential was explored using model hydrophobic drugs/dyes.[20] The use of diglycerol as a core as well as a spacer is based on the fact that it is known to be non-toxic, hydrophilic, has a good bioavailability and its precursor glycerol is an abundant by-product of oleochemical and biodiesel industry.[21–23] In order to strengthen the flexibility and hydrophobicity, C_{12} and C_{15} alkyl chains were assimilated that can facilitate the formation of hydrophobic cavities for the external guest candidates in the aqueous medium. For aqueous solubility, biocompatible mPEG (M_n: 750/1000) units were incorporated in the amphiphiles. Though the self-assembly of PEG based Gemini amphiphiles have been studied earlier for drug delivery, but the study is limited to only a limited number of nanocarriers.[24–28] Herein, the synthesis of novel non-ionic Gemini amphiphiles, investigation of their self-assembly behaviour and application as nanotransporter in biomedicine is reported. To the best of our knowledge, the threadlike assemblies have never been reported for dermal drug delivery.

2. Experimental section

The ^{1}H & ^{13}C NMR spectra of the synthesised compounds were recorded on JEOL 400 MHz and 100.5 MHz spectrometer and referencing was done using deuterated solvent residual peak. The different molecular weights M_w, M_n and M_z of the nanocarriers were determined using Agilent GPC system which consist of PLgel based columns and Agilent 1100 pump (for more detail about experimental procedure see the ESI†).

2.1 Synthetic details

Gemini amphiphiles (**AM-C$_a$-P$_b$**) (*a* is number of carbons in alkyl chain and *b* is the molecular weight of PEG unit) were synthesized *via* Cu(I) catalyzed Huisgen 1,3-dipolar cycloaddition reaction, first the hydrophilic and hydrophobic units were synthesized following Schemes 1 and 2 and the two moieties were then coupled together (Scheme 3).

2.1.1 Oxybis(2-azidopropane-1,3-diyl)diacetate (4). Compound **4** was synthesized by following the established procedure[29] *i.e.* azidation of compound **3** using sodium azide (1.27 g, 7 equiv., 19.53 mmol) in dimethylformamide (10 mL). The reaction mixture was stirred for 24 h at 80 °C. After completion of the reaction DMF was evaporated and the reaction mixture was extracted with chloroform (3 × 20 mL). The organic layer was dried over anhydrous sodium sulphate. The crude product obtained after evaporation of solvent was then

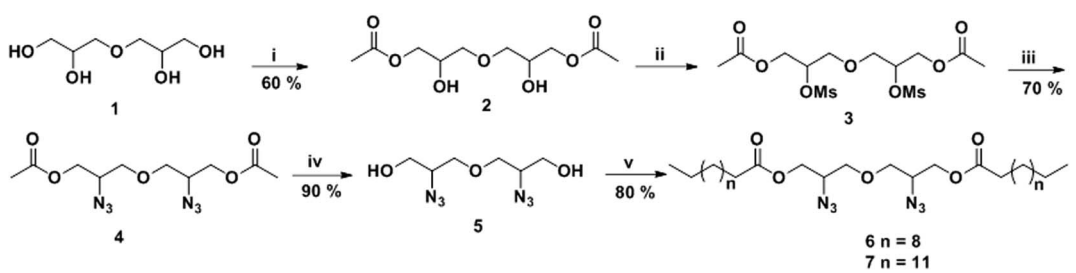

Scheme 1 Synthesis of hydrophobic moiety; reagents and conditions: (i) vinyl acetate, Novozym 435, tetrahydrofuran (THF) solvent, 30 °C, 24 h; (ii) methanesulfonyl chloride (MsCl), triethyl amine (TEA), dichloromethane (DCM), 0–25 °C, 12 h; (iii) sodium azide (NaN_3), dimethylformamide (DMF), 80 °C, 24 h; (iv) Dowex 50wx8, methanol, reflux, 12 h; (v) *n*-alkyl carboxylic acid, EDAC·HCl, *N*,*N*-dimethylaminopyridine (DMAP), dichloromethane (DCM), 25 °C, 12 h.

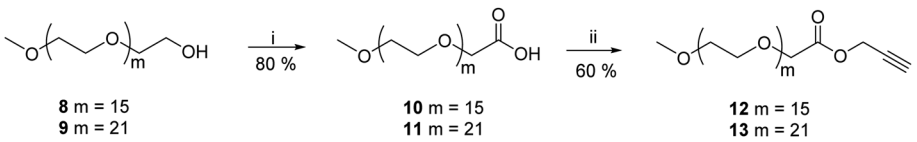

Scheme 2 Synthesis of hydrophilic moiety; reagents and conditions: (i) potassium permanganate ($KMnO_4$), sodium hydroxide (NaOH), water, 80 °C, 24 h; (ii) potassium carbonate (K_2CO_3), propargyl bromide, DMF, 50 °C, 12 h.

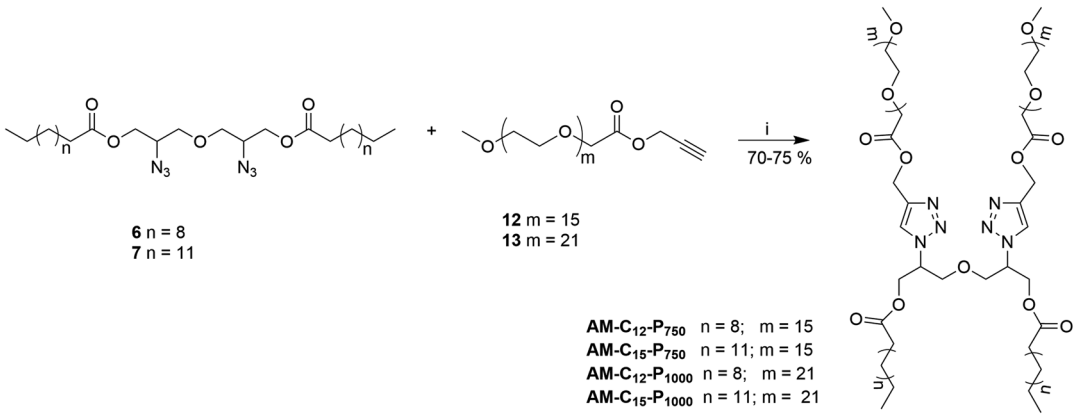

Scheme 3 Synthesis of Gemini amphiphiles; reagents and conditions: (i) $CuSO_4$, sodium-ascorbate, THF, 50 °C, 24 h.

purified by column chromatography in ethyl acetate and hexane mixture.[29] Compound **4** was obtained in 70% yield (0.586 g) as a yellow colored viscous oil. IR (KBr) ν_{max}: 2918, 2860, 2150, 1756, 1352, 1253, 1107 cm^{-1}; ^1H NMR (400 MHz, $CDCl_3$): δ 2.07 (s, 6H, $-COCH_3$), 3.58–3.61 (m, 4H, 2 × H-3), 3.76–3.77 (m, 2H, 2 × H-2), 4.07–4.22 (m, 4H, 2 × H-1); ^{13}C NMR (100.5 MHz, $CDCl_3$): δ 20.75 ($-CH_3$), 59.46 (C-2), 63.38 (C-1), 71.04 (C-3), 170.59 (–C═O).

2.1.2 Synthesis of 3,3′-oxybis(2-azidopropan-1-ol) (5). Compound **5** was obtained by hydrolysis of acetoxy group in compound **4** (1 g, 1 equiv., 3.33 mmol) using Dowex 50wx8 (500 mg) and methanol (10 mL) as a solvent. The reaction was stirred for 12 h at 50 °C. After 12 h Dowex was filtered out and the methanol was evaporated. The compound was obtained as a viscous liquid (0.498 g, 90% yield).

2.1.3 General procedure for the synthesis of oxybis(2-azidopropane-1,3-diyl)didodecanoate (6)/oxybis(2-azidopropane-1,3-diyl)dipentadecanoate (7). To the stirred solution of compound **5** (300 mg, 1 equiv., 1.39 mmol) and dodecanoic acid/pentadecanoic acid (610 mg/721 mg, 2.2 equiv., 3.04/3.01 mmol) in anhydrous dichloromethane (5 mL), *N*-(3-dimethylaminopropyl)-*N*-ethyl-carbodiimide hydrochloride (EDC·HCl) (3 equiv., 798 mg, 4.16 mmol) was added followed by addition of 4-dimethylaminopyridine (DMAP) (1.2 equiv., 203 mg, 1.63 mmol) at 0 °C. The reaction mixture was stirred at 25 °C for 12 h. After completion of the reaction DCM was evaporated under reduced pressure and the crude product so obtained was extracted with ethyl acetate (3 × 50 mL). The organic layer was dried over anhydrous sodium sulphate and then the solvent was evaporated and the compound was purified by column chromatography using a mixture of ethyl acetate and hexane to yield the target compound.

2.1.3.1 Oxybis(2-azidopropane-1,3-diyl)didodecanoate (6). Hydrophobic chain was incorporated on the diglycerol core by esterification of compound **5** with dodecanoic acid to yield compound **6** as a yellow colored viscous oil (0.645 g, 80% yield). IR (KBr) ν_{max}: 2923, 2854, 2098, 2100, 1600, 1460, 1263, 1120 cm^{-1}; ^1H NMR (400 MHz, $CDCl_3$): δ 0.87 (t, 6H, $J = 6.8$ Hz, H-12′), 1.25–1.28 (m, 32H, H-4′ to H-11′), 1.59–1.64 (m, 4H, H-3′), 2.34 (t, 4H, $J = 7.6$ Hz, H-2′), 3.59–3.62 (m, 4H, 2 × H-1), 3.65–3.77 (m, 2H, 2 × H-2), 4.09–4.26 (m, 4H, 2 × H-3); ^{13}C NMR (100.5 MHz, $CDCl_3$): δ 14.18 (C-12′), 22.75 (C-11′), 24.90, 29.31, 29.40, 29.52, 29.70, 31.97, 34.12 (C-2′ to 10′), 59.63 (C-2), 63.24 (C-1), 71.10 (C-3), 173.42 (C-1′); HRMS: *m*/*z* $[M + H]^+$ calculated for $C_{30}H_{56}N_6O_5$: 581.4349; found: 582.4684.

2.1.3.2 Oxybis(2-azidopropane-1,3-diyl)dipentadecanoate (7). Pentadecanoic acid was attached to compound **5** giving compound **7** as a yellow coloured viscous oil (0.738 g, 80% yield). IR (KBr) ν_{max}: 2930, 2860, 2150, 1711, 1461, 1285, 1120 cm^{-1}; ^1H NMR (400 MHz, $CDCl_3$): δ 0.87 (t, 6H $J = 6.8$ Hz, H-15′), 1.25–1.28 (m, 44H, H-4′–H-14′), 1.61–1.64 (m, 4H, H-3′), 2.34 (t, 4H, $J = 7.6$ Hz, H-2′), 3.56–3.65 (m, 4H, 2 × H-1), 3.78–3.819 (m, 2H, 2 × H-2), 4.12–4.26 (m, 4H, 2 × H-3); ^{13}C NMR (100.5 MHz, $CDCl_3$): δ 14.25 (C-15′), 22.77 (C-14′), 29.19, 29.44, 29.54, 29.68, 29.73, 29.77, 32.00 (C-3′ to C-13′), 34.13 (C-2′), 59.63 (C-2), 63.23 (C-1), 71.13 (C-3), 173.45 (C-1′); HRMS: *m*/*z* $[M + H]^+$ calculated for $C_{36}H_{68}N_6O_5$: 664.5251; found: 665.5289.

2.1.4 General procedure for the synthesis of prop-2-yn-1-yl(methoxypoly(oxyethylene)oate) (12/13). mPEG-750/1000 acid (**10**/**11**) (500 mg, 1 equiv., 0.64 mmol) was taken in 100 mL RB flask and dissolved in dimethylformamide (10 mL) followed by the addition of potassium carbonate (310/234 mg, 3.5 equiv., 2.24/1.69 mmol) and the solution kept stirring for 30 min.

Propargyl bromide (160 mg) was then added and the reaction mixture stirred for 12 h at 50 °C. On completion of the reaction DMF was evaporated and the crude product was extracted with chloroform (3 × 50 mL). The organic layer was dried over anhydrous sodium sulphate and the solvent was then evaporated on a rotary evaporator. The compound (**12**/**13**) was purified by column chromatography using silica gel (mesh size 200–300) in the mixture of chloroform and methanol.

*2.1.4.1 Prop-2-yn-1-yl(methoxypoly(oxyethylene)oate) (**12**).* The titled compound **12** was obtained as a yellow colored viscous liquid (0.314 g, 60% yield). IR (KBr) ν_{max}: 3330, 2920, 2880, 2130, 1756, 1600, 1461, 1210, 1120 cm^{-1}; ^1H NMR (400 MHz, $CDCl_3$): δ 2.45 (s, 1H, H-3), 3.16 (s, 3H, $-OCH_3$), 3.19–3.54 (m, $-OCH_2-CH_2$ of mPEG region), 3.96–4.03 (m, 2H, H-2′), 4.55–4.56 (m, 2H, H-1); ^{13}C NMR (100.5 MHz, $CDCl_3$): δ 52.09 (C-1), 58.92 ($-OCH_3$), 68.38 (C-2′), 70.47, 70.90, 71.84 ($-OCH_2CH_2-$), 75.63 (C-3), 169.67 (C=O).

*2.1.4.2 Prop-2-yn-1-yl(methoxypoly(oxyethylene)oate) (**13**).* Compound **13** was obtained as a yellow colored viscous liquid (0.311 g, 60% yield). IR (KBr) ν_{max}: 3324, 2920, 2880, 2130, 1756, 1603, 1461, 1210, 1123 cm^{-1}; ^1H NMR (400 MHz, $CDCl_3$): δ 2.48 (s, 1H, H-3), 3.27 (s, 3H, $-OCH_3$), 3.53–3.54 (m, $-OCH_2-CH_2$ of mPEG region), 4.11 (s, 2H, H-2′), 4.64 (s, 2H, H-1); ^{13}C NMR (100.5 MHz, $CDCl_3$): δ 52.16 (C-1), 59.01 ($-OCH_3$), 68.46 (C-2′), 70.48, 70.57, 70.99, 71.91 ($-OCH_2CH_2$), 75.54 (C-3), 169.73 (C=O).

2.1.5 General procedure for the synthesis of compound AM-C_{12}-P_{750}/AM-C_{15}-P_{750}/AM-C_{12}-P_{1000}/AM-C_{15}-P_{1000}. The hydrophobic moiety (**6**/**7**) (25 mg, 1 equiv., 43/36 μmol) and the hydrophilic moiety (**12**/**13**) (110/90 mg, 2.5 equiv., 104/92 μmol) were taken together in a 10 mL round bottom flask and dissolved in tetrahydrofuran (THF) (3 mL). Copper sulphate (4.2/3.7 mg, 0.4 equiv., 17/15 μmol) and sodium ascorbate (7.0/5.8 mg, 0.8 equiv., 33/29 μmol) were taken in a sample vial and dissolved in water (1 mL), this solution was then added to the reaction mixture. Reaction was kept for stirring for 24 h at 50 °C, the progress of the reaction was monitored by TLC. After completion of the reaction, THF was evaporated under reduced pressure and the residual product then extracted with chloroform (3 × 20 mL). The organic layer was dried over anhydrous sodium sulphate and the solvent was evaporated by using a rotary evaporator. The crude product so obtained was purified by column chromatography using the mixture of chloroform and methanol. The amphiphiles (**AM-C_{12}-P_{750}**/**AM-C_{15}-P_{750}**/**AM-C_{12}-P_{1000}**/**AM-C_{15}-P_{1000}**) were obtained in 70–75% yield.

*2.1.5.1 Amphiphile **AM-C_{12}-P_{750}**.* The click reaction of compound **6** with compound **12** by following general procedure gives amphiphile **AM-C_{12}-P_{750}** as a yellow colored viscous oil (0.070 g, 75% yield). IR (KBr) ν_{max}: 2818, 2769, 1756, 1620, 1211 cm^{-1}; ^1H NMR (400 MHz, $CDCl_3$): δ 0.86 (t, 6H, J = 7.2 Hz, H-12′), 1.23 (s, H-4′–H-11′), 1.52–1.55 (m, 4H, H-3′), 2.25 (t, 4H, J = 6.4 Hz, H-2′), 3.36 (s, 6H, $-OCH_3$), 3.52–3.74 (m, $-OCH_2CH_2$ of PEG 750 region), 3.82–3.88 (m, 4H, H-5″), 4.16–4.19 (m, 4H, 2 × H-1), 4.40–4.43 (m, 4H, 2 × H-3), 4.79–4.90 (m, 2H, H-2), 5.27 (d, 4H, J = 2.8 Hz, H-3″), 7.63–7.68 (m, 2H, H-1″); ^{13}C NMR (100.5 MHz, $CDCl_3$): δ 14.18 (C-12′), 22.73 (C-11′), 24.78, 29.11, 29.28, 29.39, 29.50, 29.65, 31.96, 33.93 (C-3′–C-10′), 59.09 ($-OCH_3$), 59.58, 62.26, 68.52, 70.60, 70.98, 71.98, 124.10 (C-1″), 142.42 (C-2″), 170.48 (C-4″), 173.09 (C-1′); GPC (THF, 1.2 mL min^{-1}): M_w = 2506.5 g mol^{-1}, M_n = 2425.3 g mol^{-1}, M_z = 2582.3 g mol^{-1}, polydispersity index (PDI) = 1.033.

*2.1.5.2 Amphiphile **AM-C_{15}-P_{750}**.* The cycloaddition reaction between compounds **7** and **12** gives amphiphile **AM-C_{15}-P_{750}** as a yellow colored viscous oil (0.064 g, 70% yield). IR (KBr) ν_{max}: 2918, 2860, 1756, 1608, 1285 cm^{-1}; ^1H NMR (400 MHz, $CDCl_3$): δ 0.85 (t, 6H, J = 7.2 Hz, H-15′), 1.22 (s, H-4′–H-14′), 1.50–1.53 (m, 4H, H-3′), 2.2 (t, 4H, J = 7.2 Hz, H-2′), 3.35 (s, 6H, $-OCH_3$), 3.51–3.72 (m, $-OCH_2CH_2$ of PEG), 3.85–3.87 (m, 4H, H-5″), 4.14–4.17 (m, 4H, 2 × H-1), 4.39–4.42 (m, 4H, 2 × H-3), 4.87–4.90 (m, 2H, 2 × H-2), 5.25–5.26 (m, 4H, H-3″), 7.61–7.66 (m, 2H, H-1″); ^{13}C NMR (100.5 MHz, $CDCl_3$): δ 14.20 (C-15′), 22.75 (C-14′), 24.78, 29.12, 29.30, 29.42, 29.75, 31.98, 33.93 (C-3′–C-10′), 57.76, 59.10 ($-OCH_3$), 62.27, 68.53, 70.094, 70.99, 71.98, 124.14 (C-1″), 142.42 (C-2″), 170.46 (C-4″), 173.08 (C-1′); GPC (THF, 1.2 mL min^{-1}): M_w = 2537.1 g mol^{-1}, M_n = 2474.1 g mol^{-1}, M_z = 2596.5 g mol^{-1}, polydispersity index (PDI) = 1.025.

*2.1.5.3 Amphiphile **AM-C_{12}-P_{1000}**.* The azide–alkyne cycloaddition reaction of compounds **6** and **13** gives amphiphile **AM-C_{12}-P_{1000}** as a yellow colored viscous oil (0.081 g, 70% yield). IR (KBr) ν_{max}: 2950, 2859, 1756, 1591, 1352, 1253 cm^{-1}; ^1H NMR (400 MHz, $CDCl_3$): δ 0.86 (t, 6H, J = 7.2 Hz, H-12′), 1.23–1.28 (m, H-4′–H-11′), 1.52–1.54 (m, 4H, H-3′), 2.25 (t, 4H, J = 7.2 Hz, H-2′), 3.36 (s, 6H, $-OCH_3$), 3.52–3.741 (m, $-OCH_2CH_2$ of PEG), 3.80–3.88 (m, 4H, H-5″), 4.16–4.18 (m, 6H, 2 × H-1–2 × H-2), 4.43–4.45 (m, 4H, 2 × H-3), 4.94–5.26 (m, 4H, H-3″), 7.62–7.67 (m, 2H, H-1″); ^{13}C NMR (100.5 MHz, $CDCl_3$): δ 14.11 (C-12′), 22.66 (C-11′), 29.04, 29.31, 29.43, 29.58, 31.88 (C-3′–C-10′), 51.77, 59.02 ($-OCH_3$), 61.68, 68.41, 68.62, 70.05, 70.26, 70.56, 70.92, 71.93, 72.63, 124.00 (C-1″), 142.37 (C-2″), 170.39, 170.89 (C-4″), 172.99 (C-1′); GPC (THF, 1.2 mL min^{-1}): M_w = 2578.9 g mol^{-1}, M_n = 2661.3 g mol^{-1}, M_z = 2736.3 g mol^{-1}, polydispersity index (PDI) = 1.032.

*2.1.5.4 Amphiphile **AM-C_{15}-P_{1000}**.* The click cycloaddition reaction of compound **7** with **13** gives amphiphile **AM-C_{15}-P_{1000}** as a yellow colored viscous oil (0.729 g, 70% yield). IR (KBr) ν_{max}: 2860, 1756, 1680, 1352 cm^{-1}; ^1H NMR (400 MHz, $CDCl_3$): δ 0.84 (t, 6H, J = 7.2 Hz, H-15′), 1.21–1.24 (m, H-4′–H-14′), 1.50–1.51 (m, 4H, H-3′), 2.23 (t, 4H, J = 6.4 Hz, H-2′), 3.35 (s, 6H, $-OCH_3$), 3.51–3.72 (m, $-OCH_2CH_2$ of PEG), 4.14–4.15 (m, 4H, H-5″), 4.16–4.18 (m, 4H, 2 × H-2 & H-1) 4.39–4.43 (m, 2H, H-1), 4.71–4.72 (m, 2H, H-3), 4.85–4.90 (m, 2H, H-3), 5.25 (d, 4H, J = 2.8 Hz, H-3″), 7.61–7.65 (m, 2H, H-1″); ^{13}C NMR (100.5 MHz, $CDCl_3$): δ 14.18 (C-15′), 22.73 (C-14′), 24.77, 29.11, 29.70, 31.97, 33.93 (C-3′–C-10′), 51.85, 57.76, 59.07 ($-OCH_3$), 59.58, 61.68, 62.27, 68.52, 68.67, 70.59, 70.97, 71.97, 72.83, 124.14 (C-1″), 142.43 (C-2″), 170.47 (C-4″), 170.98, 173.10 (C-1′); GPC (THF, 1.2 mL min^{-1}): M_w = 3154.4 g mol^{-1}, M_n = 3220.4 g mol^{-1}, M_z = 3292.9 g mol^{-1}, polydispersity index (PDI) = 1.021.

3. Results and discussion

mPEG (M_n: 750 and 1000 g mol^{-1}) and diglycerol based Gemini amphiphiles were successfully synthesised *via* Cu(I) catalyzed "1,3-dipolar cycloaddition reaction" as shown in Schemes 1–3.

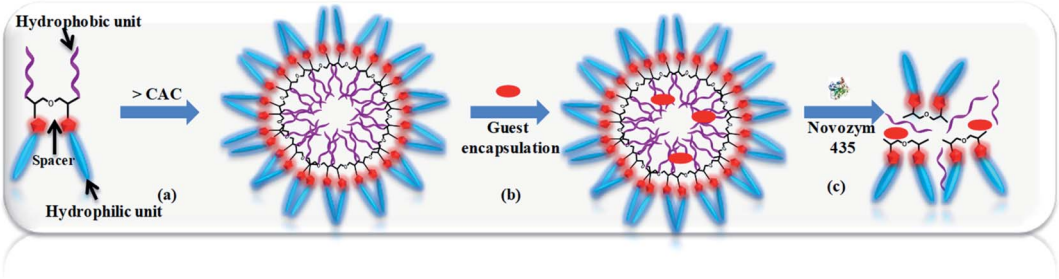

Fig. 1 (a) Schematic representation of amphiphiles which self-assemble in aqueous medium; (b) hydrophobic guest encapsulation in the cavity of nanostructures and; (c) release of guest molecules in the presence of Novozym 435.

All the four amphiphiles along with their intermediates were fully characterised by various spectroscopic techniques, *i.e.* nuclear magnetic resonance (NMR), infrared spectroscopy (IR), high resolution mass spectrometry (HRMS) and gel permeation chromatography (GPC). The physicochemical properties and supramolecular aggregation behaviour of the nanocarriers synthesised was studied by ultraviolet (UV), fluorescence, dynamic light scattering (DLS) and their morphology was studied by transmission electron microscopy (TEM). Our interest is to explore the role of hydrophobic and hydrophilic units on the self-organization, *i.e.* size, morphology, encapsulation of guest molecules and applications in biomedicine. Fig. 1 shows systematically the self-organization of amphiphiles in aqueous medium, hydrophobic guest encapsulation, and the release of the guest in the presence of Novozym 435.

3.1 Synthesis and characterization

The hydrophobic constituents were synthesised by using 3,3′-oxybis(propane-1,2-diol) (**1**) as a core unit which was synthesised by following the earlier reported procedure by our group.[30] The primary hydroxyl groups of diglycerol (**1**) were selectively acetylated using vinyl acetate in the presence of immobilized *Candida antarctica* lipase (Novozym 435) by the standardized bio-catalytic procedure to yield diacetyl derivative (**2**).[29,31–33] The observance of a peak at 1700 cm^{-1} in the IR spectrum accounts for the carbonyl group in the molecule (**2**). Subsequently, the secondary hydroxyl groups of compound **2** were substituted with azido groups *via* mesylation followed by azidation using sodium azide in a nucleophilic substitution reaction to yield compound **4**. The appearance of characteristic peak at 2150 cm^{-1} in the IR spectrum corroborates the presence of azide group in compound **4**. This compound was then subjected to acetyl deprotection reaction using Dowex 50wx8 in methanol to furnish compound **5** being used as a central core. The disappearance of peak at 1700 cm^{-1} corresponding to the carbonyl of ester along with the appearance of peak at 3300 cm^{-1} for the hydroxyl groups in the IR spectrum of **5** further confirms the deprotection reaction. The hydrophobic alkyl chains (C_{12}/C_{15}) were then incorporated on to the core (**5**) *via* ester linkage in the presence of EDC·HCl as a coupling reagent and *N*,*N*-dimethylaminopyridine (DMAP) as a base (Scheme 1). The obtained hydrophobic precursors **6** and **7** were completely characterised using spectroscopic techniques, *i.e.* ^1H & ^{13}C NMR, HRMS, *etc.* The appearance of characteristics triplet at δ 0.87 ppm (J = 6.8 Hz) for six protons along with the other methylene protons in the range of 1.25–1.28 ppm in the ^1H NMR spectrum confirms the coupling of alkyl chain with the diglyceryl core **5**.

Furthermore, the synthesis of PEG based hydrophilic moiety involves the oxidation of mPEG (M_n: 750 and 1000) using potassium permanganate and sodium hydroxide to yield the corresponding acid (**10**/**11**).[34] The acid was then converted to propargyl ester (**12**/**13**) by reacting it with propargyl bromide. The observance of a peak at 2.48 ppm for the terminal acetylenic proton along with the triplet at δ 4.64 ppm for methylene protons in the ^1H NMR spectrum confirmed the presence of propargyl moiety in the hydrophilic scaffolds. The appearance of a sharp peak at 2130 cm^{-1} for alkyne group in the IR spectrum further supports the formation of product (Scheme 2).

The target amphiphiles were then synthesised by coupling the hydrophobic diazide (**6**/**7**) and the mPEG alkyne (**12**/**13**) using copper sulphate salt and sodium ascorbate in THF and water mixture (3 : 1) resulting in the formation of non-ionic Gemini amphiphiles (Scheme 3). The occurrence of click coupling was established by the disappearance of the peak for the acetylenic proton observed in the precursor **12**/**13** at around δ 2.48 ppm. Further support for the synthesis of amphiphiles was drawn by the appearance of the peak in the range of 7.5–8.0 ppm corresponding to the triazolyl ring protons in ^1H NMR spectrum.

3.2 Physicochemical characterization of synthesised nanocarriers and self-assembly behaviour of amphiphile in aqueous solution

Diglycerol based amphiphiles synthesised herein were observed to be able to self-assemble in aqueous solution to form aggregates of various morphologies. The critical micellar concentration of the amphiphiles was calculated by fluorescence spectroscopic technique using the dye Nile red as a fluorescent probe. The particle size of the amphiphiles was determined using DLS instrument. The morphology of aggregates was established by the TEM of the amphiphiles. The substituent details of all the synthesised amphiphiles are shown below (Fig. 2).

3.2.1 Determination of critical aggregation concentration (CAC) using fluorescence spectrometry. Amphiphilic solutions

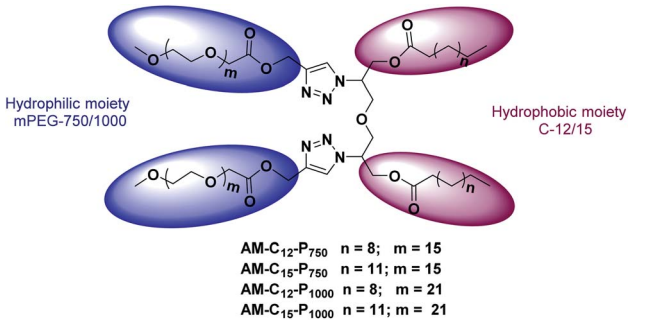

Fig. 2 Constituent details of the synthesised Gemini amphiphiles.

of different concentrations were prepared and then allowed to encapsulate the fixed amount of dye and the fluorescence data of the solutions recorded. The fluorescence intensity of Nile red was significantly enhanced at a particular concentration obtained by plotting the fluorescence intensity of encapsulated Nile red *versus* logarithmic amphiphilic concentration (Fig. 3). Such a change is due to the presence of dye in a hydrophobic surrounding created by the self-assembled amphiphiles. The breaking point in the plot denotes the CAC values of amphiphiles. The CAC of the amphiphiles was found to be in the order of 10^{-4} M. Amongst all the amphiphiles synthesized, the **AM-C_{15}-P_{750}** functionalised with the C-15 alkyl chain and mPEG 750 has lower CAC (Table 1). The critical aggregation concentration plots of the amphiphiles suggested that CAC value of amphiphiles having smaller mPEG (M_n: 750 g mol^{-1}) unit decreases with the increase in the length of the alkyl chain, whereas in case of amphiphiles with larger mPEG unit *i.e.* M_n: 1000 g mol^{-1}, CAC value increases with increasing the length of alkyl chain.

3.2.2 DLS measurements and TEM analysis. The aggregation behaviour of the synthesised amphiphiles was studied in aqueous solution at the concentration of 5 mg mL^{-1} using DLS. The DLS measurements of amphiphiles **AM-C_{12}-P_{750}**, **AM-C_{15}-P_{750}**, **AM-C_{12}-P_{1000}** and **AM-C_{15}-P_{1000}** were carried at the molar concentration of are 2.347, 2.258, 1.901, 1.842 mM, respectively. The size distribution profile of amphiphiles was found to be bimodal in intensity which signifies the size of aggregates and assembled aggregates whereas volume and number distribution plots having monomodal nature with the diameter of the formed aggregates in the range of 10 nm demonstrated that the smaller particles are prominent in aqueous solution. The plot of intensity, volume and number distribution of amphiphiles is shown in Fig. 4. The amphiphiles self-assemble into nano sized species formed in the aqueous solution having a particle size in the range 8–13 nm (Table 1). Aggregation behaviour and morphology of the nanostructured architectures formed for amphiphiles **AM-C_{15}-P_{750}** and **AM-C_{12}-P_{1000}** were analysed further by the TEM at a concentration of 5 mg mL^{-1} in aqueous solution. TEM micrographs of amphiphile **AM-C_{15}-P_{750}** depicted the population of small sized threadlike aggregates. On the other hand, the formation of spherical micelles (black arrowheads) and some threadlike aggregates (white arrowheads) were observed in the images of the aqueous solution of amphiphile

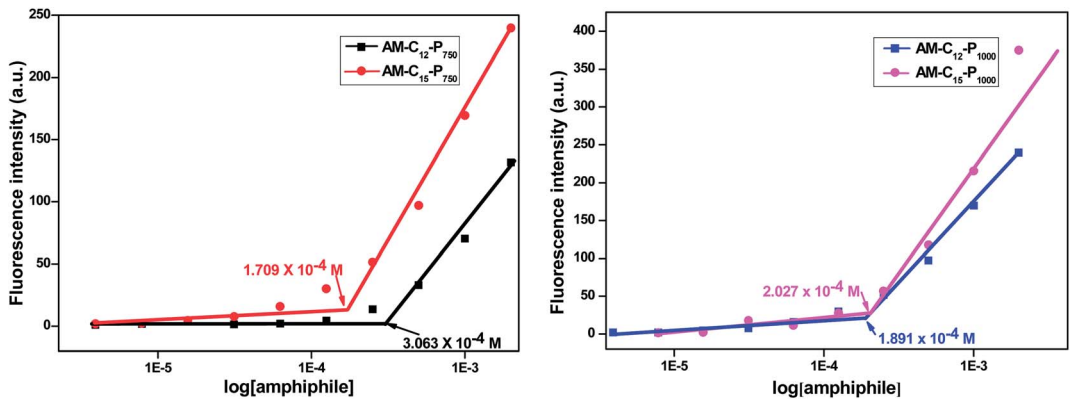

Fig. 3 CAC plot of Gemini amphiphiles.

Table 1 CAC, DLS and HLB data of amphiphiles

		DLS size [d, nm] (average value)			
Amphiphile	CAC [M]	Intensity	Volume	Number	HLB[a] $= 20 \times M_h{}^c/M_w{}^b$
AM-C_{12}-P_{750}	$3.063 \pm 0.5 \times 10^{-4}$	13.52	11.72	10.16	12.81
AM-C_{15}-P_{750}	$1.709 \pm 0.8 \times 10^{-4}$	9.83	10.08	8.71	12.66
AM-C_{12}-P_{1000}	$1.891 \pm 0.6 \times 10^{-4}$	10.16	8.62	8.62	15.68
AM-C_{15}-P_{1000}	$2.027 \pm 0.4 \times 10^{-4}$	13.23	11.56	10.08	15.20

[a] Griffin equation. [b] Molecular weight of amphiphiles determined by GPC. [c] Molecular weight of hydrophilic part.

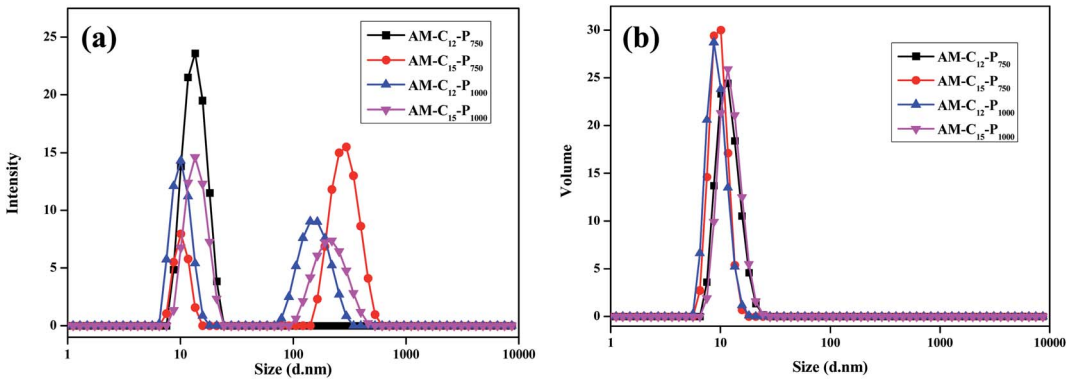

Fig. 4 DLS data for the amphiphiles, taken in water at the conc. of 5 mg mL^{-1} (a) intensity distribution graph (b) volume distribution graph.

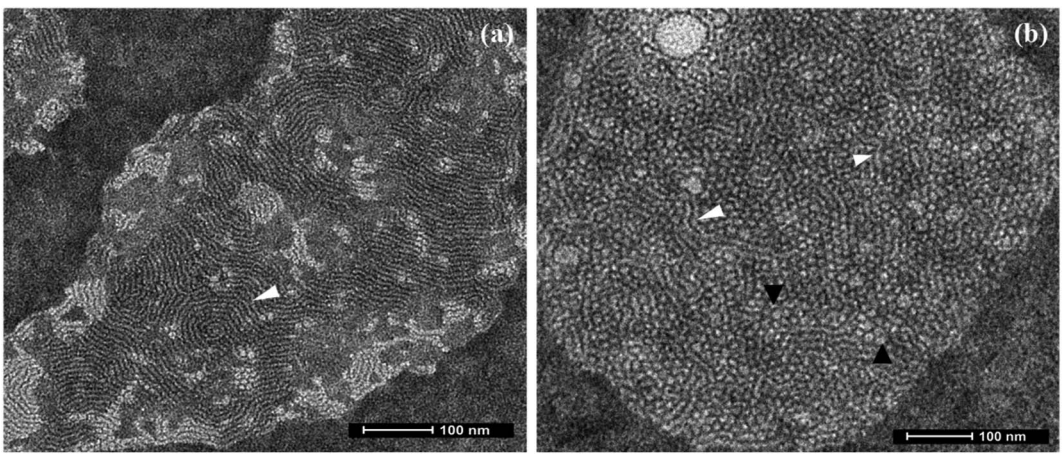

Fig. 5 TEM micrograph of amphiphile (a) **AM-C_{15}-P_{750}** and (b) **AM-C_{12}-P_{1000}** in water at the conc. of 5 mg mL^{-1}. The image of amphiphile **AM-C_{15}-P_{750}** in the aqueous solution shows the thin threadlike assemblies and amphiphile **AM-C_{12}-P_{1000}** self-assembled into the spherical micellar aggregates (black arrowheads) along with small percentage of thread-like assemblies (white arrowheads).

AM-C_{12}-P_{1000} (Fig. 5). The diameter of spherical micelles was found to be around 6 nm, which is consistent with the DLS data. DLS allows measuring the hydrodynamic diameter of aggregates, provided that they are spherical that has the same translational diffusion coefficient as the particle. That transitional diffusion coefficient will depend not only on the size of the particle core, but also depends on number of factors, out of these factors one factor is type of ions in the medium that, explains about the hydrodynamics diameter of non-spherical particles. The hydrodynamics diameter of a non-spherical particle is the diameter of a sphere that has the same translational diffusion speed as the particle, the non-spherical particle generally move with the same velocity as particles with a diameter corresponding to the smallest particle length that means by DLS we can measure the hydrodynamics diameters of non-spherical particles such as thread like aggregates.[35] Amphiphile **AM-C_{15}-P_{750}** having longer alkyl chain (C_{15}) and shorter mPEG (M_n: 750 g mol^{-1}) unit with a HLB value of 12.66 leads to the formation of threadlike nanostructures whereas amphiphile **AM-C_{12}-P_{1000}** consisting of smaller alkyl chain (C_{12}) and longer mPEG unit (M_n: 1000 g mol^{-1}) and a HLB value of 15.68 favours the formation of spherical micelles. All the studies were done in triplicate and the average value considered in the DLS measurement of the amphiphiles as shown in Table 1.

3.3 Encapsulation potential of amphiphiles for Nile red dye, nimodipine and curcumin drugs

Nile red is a hydrophobic and highly fluorescent probe that is used for the identification of the neutral lipid deposit within the cells.[36] Also, it is frequently used to evaluate the transport behaviour of the synthesised amphiphiles. Solubilisation experiments were used to explore the pertinence of the non-ionic diglycerol based Gemini amphiphiles synthesized for the dyes/drugs with the help of the thin film method.[37] The encapsulation studies were performed at a concentration of 5 mg mL^{-1} of aqueous amphiphilic solution and thin film of 0.12/0.4/0.5 mg of Nile red/nimodipine/curcumin was prepared in sample vials. The unencapsulated (free) drug/dye exist as a precipitate in the solution and was removed by filtration using 0.45 μm PTFE filter. The transport capacity, transport efficiency and encapsulation efficiency of the synthesised amphiphiles for

Table 2 Transport efficiency, transport capacity and encapsulation efficiency of amphiphiles for Nile red, nimodipine and curcumin

	Transport efficiency [mg g^{-1}]			Transport capacity [mmol mol^{-1}]			Encapsulation efficiency[a] (%)		
Amphiphile	NR[b]	NIM[c]	CUR[d]	NR	NIM	CUR	NR	NIM	CUR
AM-C_{12}-P_{750}	0.12	11.38	4.03	0.82	61.76	23.91	0.50	11.87	2.01
AM-C_{15}-P_{750}	0.60	32.23	11.03	4.26	169.78	67.99	2.49	33.57	5.52
AM-C_{12}-P_{1000}	0.19	5.14	4.19	1.55	33.03	30.55	1.03	5.36	2.09
AM-C_{15}-P_{1000}	0.25	7.38	6.12	2.14	48.88	46.04	0.80	7.69	3.06

[a] Encapsulation efficiency (%) = amount of dye encapsulated × 100/amount of dye added. [b] NR: Nile red. [c] NIM: nimodipine. [d] CUR: curcumin.

the guest molecules has been depicted in Table 2. The UV and fluorescence spectra of Nile red loaded samples were recorded in methanol as a solvent and is shown in Fig. S12 (ESI†). Amphiphile **AM-C_{15}-P_{750}** consisting of C-15 alkyl chain and mPEG 750 exhibited maximum encapsulation of Nile red followed by amphiphiles **AM-C_{15}-P_{1000}**, **AM-C_{12}-P_{1000}** and **AM-C_{12}-P_{750}**. The study indicated that amphiphiles **AM-C_{15}-P_{750}** and **AM-C_{15}-P_{1000}** having longer alkyl chain (C_{15}) showed higher encapsulation of Nile red as compared to amphiphiles with smaller alkyl chain (C_{12}). Amphiphile **AM-C_{15}-P_{750}** has the tendency to efficiently transport 0.60 mg of Nile red for 1 g of it.

Nimodipine is known as calcium channel blocker in the pharmaceutical chemistry and it was developed by Bayer AG in 1983. It consists of 1,4-dihydropyridine skeleton and is used for the treatment of cerebrovascular spasm, migraine, stroke and the neurological disorders. But it has low bioavailability due to limited aqueous solubility, which hampers its clinical usefulness.[38] In order to enhance drug efficacy nimodipine was entrapped in the self-assembled aggregates formed from the amphiphilic architectures at a concentration of 5 mg mL^{-1} by the thin film method. Quantification of the encapsulated nimodipine was carried by UV spectrophotometer following Beer Lambert's law and using molar extinction coefficient of drug in ethanol (ε 7200 M^{-1} cm^{-1} at 356 nm).[39] Amphiphile **AM-C_{15}-P_{750}** which consists of C-15 hydrophobic alkyl chain and hydrophilic mPEG 750 showed higher encapsulation efficiency as it was able to efficiently transport 32.23 mg of nimodipine for 1 g of amphiphile.

Curcumin, isolated from *Curcuma longa* is a hydrophobic compound having bi-phenolic structure. It is enriched with many pharmacological activities such as anticancer, antioxidant, anti-inflammatory, *etc.*[40,41] However, it has poor bioavailability due to its low aqueous solubility and reduced permeability across the blood–brain barrier which curtails its applicability as a drug.[42] We have successfully attempted to enhance its bioavailability by encapsulating it in the amphiphiles synthesised. Encapsulation and quantitative measurements were performed using UV-Vis spectrophotometer and taking 0.5 mg of the drug and the 5 mg mL^{-1} of amphiphilic concentration by Lambert Beer's law using a molar extinction coefficient *i.e.* ε 55 306 M^{-1} cm^{-1} at 425 nm (ref. 43) for curcumin in methanol (ESI, Fig. S13†). For curcumin too, amphiphile **AM-C_{15}-P_{750}** showed the highest encapsulation efficiency as observed earlier in the case of Nile red and nimodipine (Fig. 6).

A comparison of the quantification of encapsulation of hydrophobic guest in amphiphiles suggested that an increase in the length of the alkyl chain by keeping the identical hydrophilic unit results in an enhancement of the transport potential of amphiphiles.

3.4 Cytotoxicity study

The cytotoxicity of primary concerns in the development of efficient nano-carriers for drug delivery applications. The cytotoxicity of the synthesised amphiphilic systems were examined *in vitro* cell lines, *i.e.* HeLa cervical carcinoma cells and MCF7

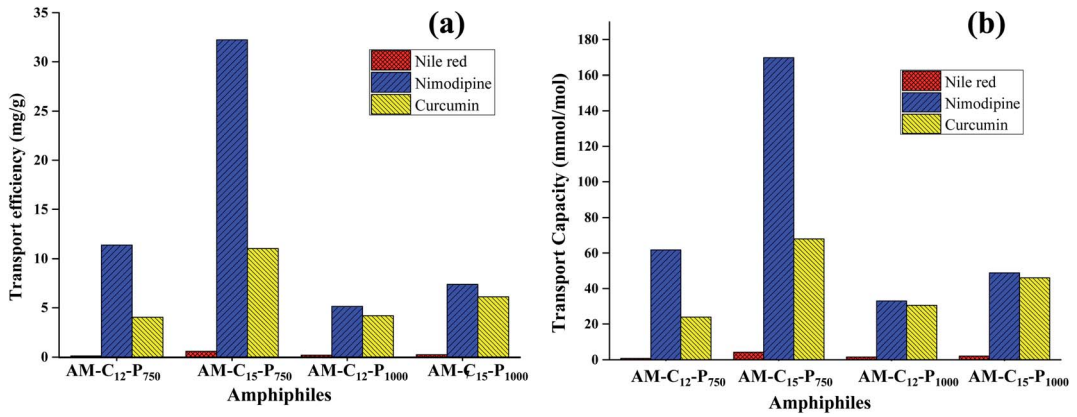

Fig. 6 Depiction of transport efficiency (a) and transport capacity (b) of amphiphiles.

breast adenocarcinoma cells because theses cell lines growing in a 2D environment gives appropriate cytotoxicity information. Both cell lines were treated with the amphiphiles at various concentrations *i.e.* 0.05, 0.1 and 0.5 mg mL^{-1} for 24 h in the CKK-8 assay. No reduction of the cell viability was observed in HeLa cells at the concentration 0.05, 0.1 and 0.5 mg mL^{-1} for the amphiphiles **AM-C_{15}-P_{750}**, **AM-C_{15}-P_{1000}** and **AM-C_{12}-P_{1000}**. Compound **AM-C_{12}-P_{750}** exhibits some cytotoxicity as the concentration reached 0.5 mg mL^{-1} though it remains non-cytotoxic at the lower concentrations. On the other hand, in MCF7 cell lines, all the amphiphiles showed little cytotoxicity at the 0.5 mg mL^{-1} concentration (Fig. 7). However, at the lower concentrations, *i.e.* 0.1 and 0.05 mg mL^{-1} these compounds were found to be non-cytotoxic. In conclusion, compounds showed higher cytotoxicity in MCF7 cell lines as compared to the HeLa cell lines. All the compounds are non-cytotoxic in both the cell lines at concentrations 0.1 and 0.05 mg mL^{-1}.

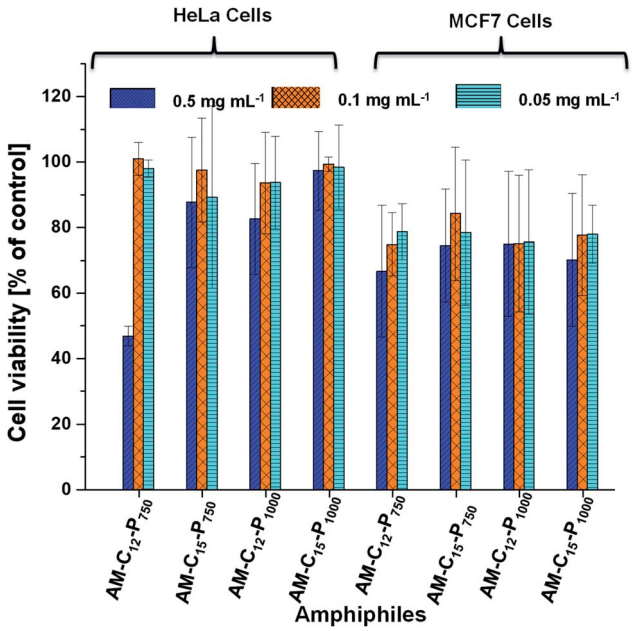

Fig. 7 The cytotoxicity profile of all amphiphiles after 24 h. Cytotoxicity of nanocarriers was determined with the help of CCK-8 assay using HeLa and MCF7 cells lines. Each bar represents the mean value of three independent experiments ($n = 3$) and the standard deviation.

3.5 Cellular uptake study

As the amphiphiles synthesised herein exhibited low toxicity in HeLa cells, the uptake profile of Nile red loaded into the amphiphiles **AM-C_{15}-P_{750}** and **AM-C_{15}-P_{1000}** was analysed by using confocal laser scanning microscopy (cLSM). Nile red was allowed to encapsulate in the amphiphilic architectures formed at a concentration of 0.5 mg mL^{-1} by following the same protocol as described earlier by our research group.[44] After 4 h a strong, intense signal was observed in the cytosol (Fig. 8) which was further increased after 24 h (ESI, Fig. S15†).

3.6 Skin penetration

The percutaneous absorption of Nile red (0.001% w/w) through human skin was investigated by loading dye into the nanostructures formed from the amphiphile **AM-C_{15}-P_{750}**. The safety evaluation issues based on the cell viability assay limited the applied dose of compound **AM-C_{15}-P_{750}** to 0.5 mg mL^{-1} in the skin penetration experiments. From the representative cLSM images of skin sections it is clear that following 18 hours

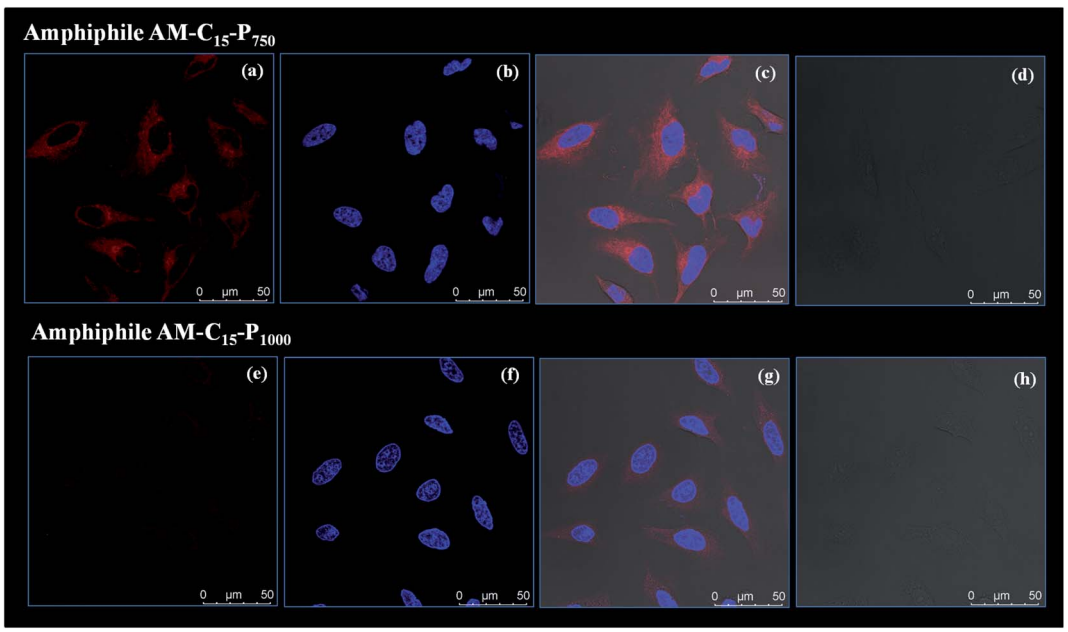

Fig. 8 Confocal laser scanning fluorescence microscopy images from HeLa cells after 4 h incubation of Nile red encapsulated in amphiphiles AM-C_{15}-P_{750} (a–d) and AM-C_{15}-P_{1000} (e–h) are shown in figure. In the images, Nile red is shown in red colour and the nucleus stained with Hoechst 33342 in blue colour. The scale bar represent 50 μm.

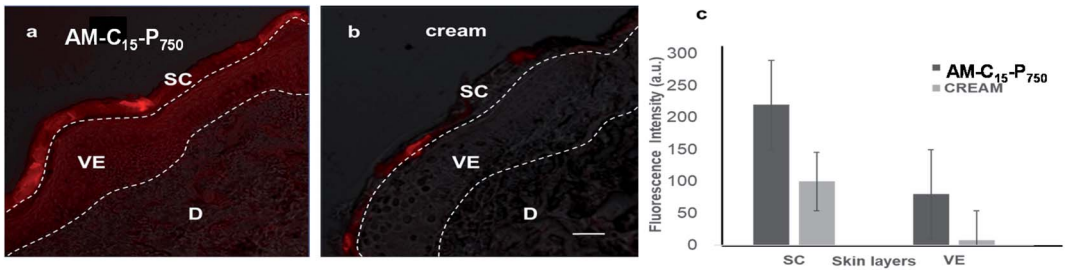

Fig. 9 The overlay of fluorescence and bright field microscopy images from human skin is represented (a) topically applied Nile red-loaded AM-C_{15}-P_{750} (0.001% w/w); (b) Nile red assimilated into base cream as a control (0.001% w/w) after 18 h; (c) fluorescence intensity of Nile red encapsulated in nano-carriers in different layers of human skin (n = 3, mean ± SEM). Where SC denotes to stratum corneum, VE is viable epidermis, and D is abbreviated for dermis layers of skin, respectively. For each image the scale bar correspond 50 μm.

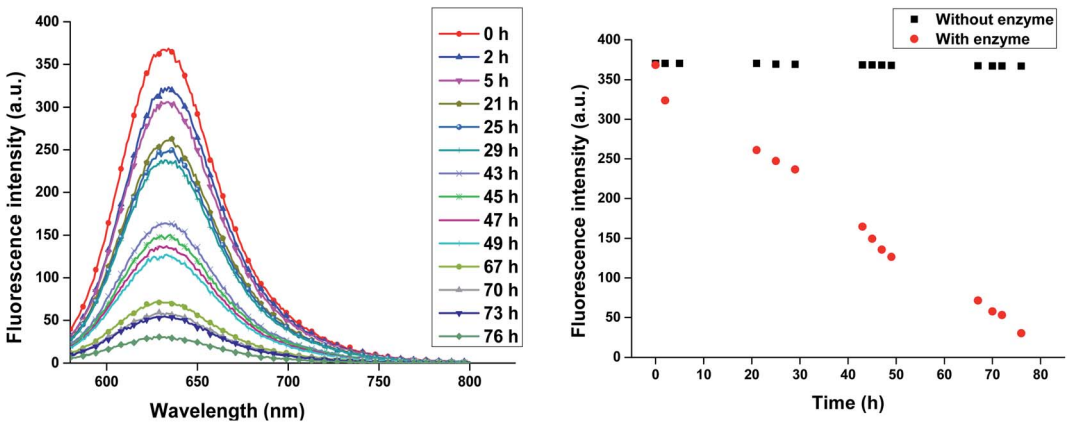

Fig. 10 Enzyme mediated release profile of encapsulated Nile red from synthesised nanocarrier AM-C_{15}-P_{750} under physiological conditions is shown in figure.

exposure of Nile red loaded **AM-C_{15}-P_{750}**, the released dye penetrated into the stratum corneum and viable epidermis layers of human skin (Fig. 9a). On the contrary, in samples treated with Nile red incorporated in a base cream, the components of which are fatty alcohol, petrolatum and mineral oil with different ratios, the fluorescence signal of Nile red was detected only in the stratum corneum (Fig. 9b). This shows that dye penetrates better the skin with the aggregates than with the cream. Since the upper layer of skin, stratum corneum, is hydrophobic and cream can diffuse efficiently. However, the inner layers of skin, viable epidermis, is hydrophilic and the synthesized amphiphilic structures can penetrate into and increase dye or drug absorption. These studies suggests that the synthesized amphiphiles can performs as penetration enhancers. Furthermore, using the Image J software, we measured quantitatively the intensity of the red fluorescence signal of Nile red (Fig. 9c). These results revealed that, in comparison with base cream, compound **AM-C_{15}-P_{750}** increases the absorption of Nile red to 2.5 folds in stratum corneum and 12 folds in the viable epidermis.

3.7 Enzyme assisted release study

Release of encapsulated therapeutics from the nano-carriers in a controlled manner results in the development of sustainable drug delivery system. We carried out the enzyme mediated release of encapsulated dye using the hydrolase enzyme *Candida antarctica* lipase (Novozym 435) under dark conditions at 37 °C. Since the amphiphiles reported here consists of ester linkages which is sensitive to enzyme, we have observed that on exposure with Novozym 435 results in the hydrolysis of amphiphiles leading to the rupture of the micellar aggregation system, thus releasing the loaded Nile red under physiological conditions causing a substantial decrease in the fluorescence, intensity of Nile red loaded nano-carrier **AM-C_{15}-P_{750}** as shown in Fig. 10. Approximately 50% release of the dye was observed after 43 h followed by 90% decay in the intensity within 76 h suggested that the encapsulated guest molecules get released within 3 days in the human body from the synthesised nano-carrier **AM-C_{15}-P_{750}**.

4. Conclusions

In conclusion, a novel series of non-ionic diglycerol based Gemini amphiphiles have been synthesised using biocompatible materials which self-assemble into supramolecular nanostructures in aqueous solution. All the synthesised nanocarriers have been characterised by spectroscopic techniques, *i.e.* IR, ^{1}H & ^{13}C NMR, HRMS and GPC. The self-assembled behaviour of

all the amphiphiles was studied using DLS and it led to the observance of formation of nanostructures at the concentration in the range of 1.7×10^{-4} to 3.0×10^{-4} M with a hydrodynamic diameter in the 8–13 nm range. Transmission electron microscopy (TEM) study of aqueous solution of amphiphile **AM-C_{15}-P_{750}** displayed the presence of threadlike structures, on the other hand amphiphile **AM-C_{12}-P_{1000}** indicated the presence of formation of spherical micelles having a diameter around 6 nm along with the formation of trace amount of threadlike assemblies. The transport potential of amphiphiles was evaluated by the fluorescence and UV-vis spectroscopic technique that indicated the better solubilisation of poorly water soluble drugs/dyes *via* encapsulation. The amphiphile **AM-C_{15}-P_{750}** exhibit the highest encapsulation of dye/drugs. Furthermore, all the amphiphiles were found to be non-cytotoxic at the concentration of 0.05 and 0.1 mg mL^{-1} in the HeLa cervix carcinoma cells and MCF7 breast adenocarcinoma cell lines with the CCK-8 assay. When the concentration is increased to 0.5 mg mL^{-1} the amphiphiles showed some cytotoxicity in both the cell lines. Confocal laser scanning microscopy demonstrated the systematic uptake of encapsulated dye in cervix carcinoma cells in 4 h. The study of dermal delivery of dye/drugs by encapsulating them with the synthesised amphiphiles showed the successful penetration of Nile red to the skin in nano-carrier **AM-C_{15}-P_{750}**. The present data showed that this study can be successfully used for biomedical applications.

Conflicts of interest

There are no conflicts to declare.

Acknowledgements

We gratefully acknowledge the BIRAC-DBT, IoE-Delhi University, and DFG, Germany the core facility BioSupraMol and Free University Berlin for financial support, and University Grants Commission, New Delhi, for providing fellowship to Ayushi Mittal. The authors would like to thank Elisa Quaas for performing cell viability measurement.

References

1 L. Shi, P. Sun and L. Zheng, *Soft Matter*, 2016, **12**, 8682–8689.
2 S. Ganta, H. Devalapally, A. Shahiwala and M. Amiji, *J. Controlled Release*, 2008, **126**, 187–204.
3 J. Ge, D. Lu, C. Yang and Z. Liu, *Macromol. Rapid Commun.*, 2011, **32**, 546–550.
4 Y. Wang, X. Wang, Y. Liu, S. Ou, Y. Tan and S. Tang, *Fuel Process. Technol.*, 2009, **90**, 422–427.
5 L. Sun, Z. Liu, L. Wang, D. Cun, H. H. Tong, R. Yan, X. Chen, R. Wang and Y. Zheng, *J. Controlled Release*, 2017, **254**, 44–54.
6 S. Zsikó, E. Csányi, A. Kovács, M. Budai-Szűcs, A. Gácsi and S. Berkó, *Sci. Pharm.*, 2019, **87**, 19.
7 H. Tanwar and R. Sachdeva, *Int. J. Pharm. Sci. Res.*, 2016, **7**, 2274.
8 J. D. Bos and M. M. Meinardi, *Exp. Dermatol.*, 2000, **9**, 165–169.
9 F. Bordi, G. Cerichelli, N. de Berardinis, M. Diociaiuti, L. Giansanti, G. Mancini and S. Sennato, *Langmuir*, 2010, **26**, 6177–6183.
10 L. Shi, F. Chen, N. Sun and L. Zheng, *Soft Matter*, 2015, **11**, 4075–4080.
11 B. Parshad, S. Prasad, S. Bhatia, A. Mittal, Y. Pan, P. K. Mishra, S. K. Sharma and L. Fruk, *RSC Adv.*, 2020, **10**, 42098–42115.
12 C. Boettcher, B. Schade and J.-H. Fuhrhop, *Langmuir*, 2001, **17**, 873–877.
13 J. Israelachvili, *Proc. Int. School Phys. Enrico Fermi Course XC*, 1985.
14 B. Kronberg and B. Lindman, *Surfactants and polymers in aqueous solution*, John Wiley & Sons Ltd., Chichester, 2003.
15 A. Mittal, Krishna, S. Prasad, P. K. Mishra, S. K. Sharma and B. Parshad, *Mater. Adv.*, 2021, **2**, 3459–3473.
16 A. K. Singh, B. N. Thota, B. Schade, K. Achazi, A. Khan, C. Böttcher, S. K. Sharma and R. Haag, *Chem.–Asian J.*, 2017, **12**, 1796–1806.
17 R. Zana, *J. Colloid Interface Sci.*, 2002, **248**, 203–220.
18 R. S. G. Krishnan, S. Thennarasu and A. B. Mandal, *J. Phys. Chem. B*, 2004, **108**, 8806–8816.
19 W. Zhao and Y. Wang, *Adv. Colloid Interface Sci.*, 2017, **239**, 199–212.
20 S. Liu, R. Sang, S. Hong, Y. Cai and H. Wang, *Langmuir*, 2013, **29**, 8511–8516.
21 B. Katryniok, H. Kimura, E. Skrzyńska, J.-S. Girardon, P. Fongarland, M. Capron, R. Ducoulombier, N. Mimura, S. Paul and F. Dumeignil, *Green Chem.*, 2011, **13**, 1960–1979.
22 P. Cintas, S. Tagliapietra, E. C. Gaudino, G. Palmisano and G. Cravotto, *Green Chem.*, 2014, **16**, 1056–1065.
23 A. Behr, J. Eilting, K. Irawadi, J. Leschinski and F. Lindner, *Green Chem.*, 2008, **10**, 13–30.
24 T. Zhou, H. Yang, X. Xu, X. Wang, J. Wang and G. Dong, *Colloids Surf., A*, 2008, **317**, 339–343.
25 P. A. FitzGerald, T. W. Davey and G. G. Warr, *Langmuir*, 2005, **21**, 7121–7128.
26 Z. Liwen and X. Honglu, *J. Dispersion Sci. Technol.*, 2008, **29**, 284–288.
27 H.-C. Kim, E. Kim, T.-L. Ha, S. W. Jeong, S. G. Lee, S. J. Lee and B. Lee, *Colloids Surf., B*, 2015, **127**, 206–212.
28 H. C. Kim, E. Kim, S. G. Lee, S. J. Lee, H. Kim and S. W. Jeong, *J. Polym. Sci., Part A: Polym. Chem.*, 2014, **52**, 582–589.
29 A. K. Singh, R. Nguyen, N. Galy, R. Haag, S. K. Sharma and C. Len, *Molecules*, 2016, **21**, 1038.
30 Parmanand, A. Mittal, A. K. Singh, K. Achazi, C. Nie, R. Haag and S. K. Sharma, *RSC Adv.*, 2020, **10**, 37555–37563.
31 S. Gupta, B. Schade, S. Kumar, C. Böttcher, S. K. Sharma and R. Haag, *Small*, 2013, **9**, 894–904.
32 A. Halldorsson, C. D. Magnusson and G. G. Haraldsson, *Tetrahedron*, 2003, **59**, 9101–9109.
33 Krishna, B. Parshad, K. Achazi, C. Böttcher, R. Haag and S. K. Sharma, *ChemMedChem*, 2021, **16**, 1457.
34 S. Prasad, K. Achazi, B. Schade, R. Haag and S. K. Sharma, *Eur. Polym. J.*, 2018, **109**, 506–522.

35 **https://warwick.ac.uk/fac/cross_fac/sciencecity/programmes/internal/themes/am2/booking/particlesize/intro_to_dls.pdf**.
36 P. Greenspan, E. P. Mayer and S. D. Fowler, *J. Cell Biol.*, 1985, **100**, 965–973.
37 E. Fleige, B. Ziem, M. Grabolle, R. Haag and U. Resch-Genger, *Macromolecules*, 2012, **45**, 9452–9459.
38 G. M. Soliman, R. Sharma, A. O. Choi, S. K. Varshney, F. M. Winnik, A. K. Kakkar and D. Maysinger, *Biomaterials*, 2010, **31**, 8382–8392.
39 B. N. Thota, H. v. Berlepsch, C. Böttcher and R. Haag, *Chem. Commun.*, 2015, **51**, 8648–8651.
40 A. Goel, A. B. Kunnumakkara and B. B. Aggarwal, *Biochem. Pharmacol.*, 2008, **75**, 787–809.
41 A. Qin, J. W. Lam, C. K. Jim, L. Zhang, J. Yan, M. Häussler, J. Liu, Y. Dong, D. Liang and E. Chen, *Macromolecules*, 2008, **41**, 3808–3822.
42 M. Kumari, M. Billamboz, E. Leonard, C. Len, C. Böttcher, A. K. Prasad, R. Haag and S. K. Sharma, *RSC Adv.*, 2015, **5**, 48301–48310.
43 S. Prasad, K. Achazi, C. Böttcher, R. Haag and S. K. Sharma, *RSC Adv.*, 2017, **7**, 22121–22132.
44 A. Mittal, A. K. Singh, A. Kumar, K. Achazi, R. Haag and S. K. Sharma, *Polym. Adv. Technol.*, 2020, **31**, 1208–1217.